Determination and Prediction of Austenite Grain Size in Relation to Product Quality of the Continuous Casting Process

Jürgen Reiter[1], Christian Bernhard[1], Hubert Presslinger[2]

[1]Christian Doppler Laboratory of Metallurgical Fundamentals of Continuous Casting Processes;
University of Leoben; Franz Josef Str. 15; 8700 Leoben; Austria
[2]voestalpine Stahl GmbH; VOEST-ALPINE-Straße3; 4031 Linz; Austria

Keywords: Continuous casting, SSCT-test, austenite grain size, grain size model

Abstract

Crack formation is a frequent problem in the continuous casting process. The formation of cracks is associated with an overcritical deformation of the strand shell in a low-ductility temperature range. Ductility troughs at elevated temperatures are attributed to the formation of precipitates, phases or segregates during cooling, particularly detrimental along grain boundaries. Besides the steel composition, process related factors, like deep oscillation marks on the strand surface associated with coarse austenite grain size, play an important role, too.

The implementation of an austenite grain size prediction model into the quality assurance system of a continuous casting machine, has therefore been the objective of a joint research work of voestalpine Stahl and the Christian Doppler laboratory for "Metallurgical Fundamentals of Continuous Casting Processes".

In a first step, slabs of different steel grades were investigated to determine the prior austenite grain size, followed by a feasibility study on the simulation of austenite grain growth under continuous casting conditions in a laboratory experiment. Following extensive experimental and metallographic work, the results served for the validation of an austenite grain size prediction model. The current work presents the applied experimental und metallographic methods, the results of the metallographic examinations as well as some results of the model.

Introduction

The formation of transverse cracks has been a vital topic since the very early days of continuous casting. Many researcher addressed this problem, for a review see e.g. [1-3]. Generally speaking, the formation of transverse cracks is associated with the overcritical deformation of the strand shell in a low-ductility temperature range. This ductility trough at elevated temperatures is attributed to the formation of precipitates, phases or segregates during cooling, particularly detrimental along austenite grain

boundaries. Besides the steel composition, process related factors, like deep oscillation marks [4-6] on the strand surface, associated with coarse austenite grain size [7, 8] play an important role, too.

The method still most frequently employed for the characterization of the hot ductility of steel is the determination of the RA (reduction of area, %) from hot tensile tests. RA can be converted to the strain to fracture or the critical strain ε_c by

$$\varepsilon_C = \ln\left(\frac{100}{100 - RA}\right) \qquad (1)$$

According to the results of Mintz [3], the minimum RA in the second ductility trough is reciprocal to the square root of the austenite grain diameter with decreasing influence of grain diameters above 300 µm. Other authors, like Ohmori and Kunitake [9], found the elongation to be reciprocal to the grain diameter for grain diameters above 100 µm. In any way, increasing austenite grain size has a remarkable influence on the ductility of steels in the ductility trough. This effect is founded in the decreasing specific grain boundary area, associated with higher precipitate density [10], the easier propagation of cracks by sliding fewer triple points [3] and the increase of the critical strain for the onset of dynamic recrystallization [11, 12]. The role of fine grains at the low temperature end of the ductility trough is rather unclear. However, fine grains encourage the formation of ferrite, which might yield to an earlier formation (at higher temperature) in large amounts, resulting in a narrow trough. All these arguments point to the importance of the austenite grain size for the ductility at elevated temperature.

Data on austenite grain growth associated with the continuous casting process are rare. Since the fundamental work of Yasumoto and Maehara et al. [4, 13, 14] the main influencing parameters are known: steel composition, the starting temperature for austenite grain growth and the cooling rate during and after solidification. For cooling rates between 0.1 and 1.5 °C/s, Miettinen [15] fitted the experimental results of Yasumoto et al. [14] using the following equation,

$$D = 21 \cdot T^{\gamma} - 3152 \cdot \left[\frac{e^{\dot{T}}}{1 + e^{\dot{T}}}\right] - 25088 \qquad (2)$$

In Eq. (2) T^{γ} denotes the highest temperature of a totally austenitic structure in °C, $\dot{T}$ is the local cooling rate of solidification in °C/s and D is the final austenite grain size in µm. It is interesting to note that the expression neglects the influence of precipitations. Under similar cooling conditions, the maximum grain size is thus found for a carbon equivalent of 0.17 wt.-%, due to the highest temperature for a totally austenitic structure in the Fe-C-system.

Data for austenite grain size is sometimes published together with the results of hot tensile tests. An example is the work of Deprez et al. [5], which demonstrates very clearly the importance of a prior melting of the probe before tensile testing in order to simulate the austenite grain formation under continuous casting conditions. After solidification and subsequent cooling at 15°C/s, the maximum grain size is measured for 0.15 and 0.2 wt.-% C steels (D = 1.2 mm), decreasing with increasing carbon content (D = 0.5 mm for 0.55 wt.-% C). The measured ductility at 900 °C shows the reverse behavior: The steels with coarse austenite grain show the lowest ductility (RA < 10%), whereas RA amounts to

more than 20% for the 0.55 wt.-% C steel. This underlines the importance of the austenite grain size for the ductility within the ductility trough.

A report on a combined experimental and numerical simulation of austenite grain growth under continuous casting conditions comes from Schwerdtfeger et al. [16]. In it, a higher sophisticated model is applied for the description of austenite grain growth, considering the influence of precipitations. According to the results of Maehara, the maximum austenite grain size was found, both in experiment and simulation, for 0.17 wt.-% C.

A recent work addresses the measurement auf austenite grain size on the continuously cast slab surfaces and the influence of increasing oscillation mark depth on the prior austenite grain size [17]. Typical average values range from 400 to 800 µm for the surface and from 600 to 1600 µm for the center of oscillation marks (0.16 – 0.20 wt.-% C steels).

The general view of the influence of steel composition on the austenite grain size is uniform: Under similar cooling conditions, a maximum has to be expected for a carbon equivalent of around 0.17 wt.-%, associated with a minimum in ductility within the ductility trough. Nevertheless, the present work started with the measurement of austenite grain size on the surface of several slabs, cast at caster No. 5 of voestalpine Stahl in Linz. The reason for the extensive metallographic examinations was to determine, in excess of existing data, a grain size distribution rather than just the average value. In doing so the relevance of laboratory tests for the continuous casting process can be ensured. A further point of interest was the characteristic of the austenite grain size over the cross section of the slab, mainly due to the influence of different cooling rates. The last point was to investigate the question, if the expected influence of the steel composition on austenite grain size from laboratory experiments proves to be applicable for slab casting conditions.

The second step in this project was the adjustment of the laboratory testing conditions, in order to simulate the grain growth in the continuous casting process under controlled conditions. The results of the experiments were used to validate the results of a coupled cooling – grain growth model. This model was finally used to calculate the grain growth on the surface of a cast slab, and the results were again compared with the austenite grain size measurement.

Grain size measurement on continuously cast slabs

For the metallographic examination, a set of 4 slabs was selected, for composition and main casting parameters see Table I. An 18 by 70 mm² area, parallel to the surface and 400 mm off the corner was ground, polished and etched. The austenite grain size was measured by the method described below. This procedure was repeated in steps of 10 mm, starting from the surface and ending in the middle of the slab or in a position where the austenite grain size could no longer be detected.

Table I. Chemical composition and casting parameter of the slabs

Steel	C [wt.-%]	Si [wt.-%]	Mn [wt.-%]	casting speed [m/min]	slab thickness [mm]	slab width [mm]
A	0,168	0,21	1,50	1,2	215	1294
B	0,185	0,22	0,69	1,2	215	1300
C	0,530	0,24	0,86	1,2	215	1171
D	0,21	0,22	1,45	1,2	215	1406

For the determination of grain size, defined standards are set in ASTM E112 and DIN EN ISO 643. Most authors apply the intercept procedure, which involves an actual count of the number of grains intercepted by a test line. This number is used to calculate the mean linear intercept length, according to the mean grain size or rather, diameter. Within the scope of the present work, a minimum number of 200 grains was marked by hand on every micrograph in a digital image analysis system. The number and area of the grains was automatically determined, and the parameters for the statistic distribution as well as the average value calculated by a statistics software.

The development of the most suitable etching technique in order to reveal the prior austenite grain boundaries in middle carbon steels was a further important prerequisite for the subsequent grain size measurement. In the literature, different etchants and methods to reveal austenite grain boundaries are reported [18-23]. Among these, ammonium persulfate (10 g ammonium persulfate, 100 ml H_2O, etching time app. 5 s), diluted nitric acid (100 ml ethanol 96%, 3 ml nitric acid 65%, etching time app. 5 s) and picric acid (170ml picric acid, together with 30 ml H_2O, 6 ml Agepon and 1.6 ml HCl, heated up to between 50 and 70 °C, and an etching time of between 2 and 5 min) proved to be the most effective etching reagents. The success of the respective etching method depends on the steel composition. One of the advantages of ammonium persulfate and nitric acid is that they are uncomplicated in production and handling, whereas picric acid has to be heated up to app. 60°C and requires careful handling because of its toxicity.

Figure 1 shows a micrograph (etchant diluted nitric acid) with clearly visible prior austenite grain boundaries at different stages of the grain size analysis. The bright phase on the left micrograph is pro-eutectoid ferrite, formed during the γ/α transition, and thus characterizing the austenite grain size near the A_3 temperature. In the middle, the micrograph is overlaid with the network of the manually drawn grain boundaries. On the right side, the digital image analysis software has identified the single grains. The size of each grain is stored in a table, which is further processed in a statistic software. Based on this measurement, the parameters for the most suitable statistical distribution and the mean grain size can be calculated.

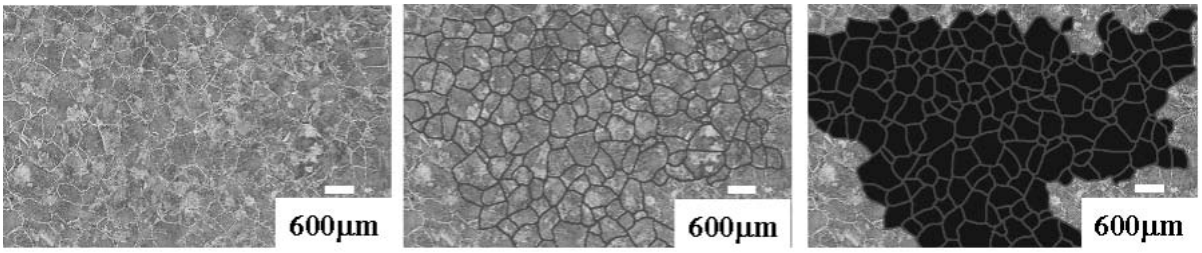

Figure 1: Evaluation of the micrograph (Experiment; 0.4 wt.-%C; diluted nitric acid; 1mm depth)

Figure 2 gives an example of the grain size distribution near the surface for slab A and slab C. The measured grain size distribution fits with an extrema distribution. The average grain size amounts to 0.76 mm² for steel A and 0.32 mm² for steel C. Assuming a round grain, the corresponding diameter would be 0.98 resp. 0.58 mm. The 0.98 mm for steel A and the measured value of 0.72 mm for steel B with a similar composition match well with the published data by Weissgerber et al.[17]. As expected from the results from literature, the maximum grain size is found for a carbon equivalent near 0.17 wt.-%, and the grain size of the higher carbon slab C is clearly lower. It should be noticed that each slab was cast with a different secondary cooling strategy. The effect of the steel composition is superimposed with the effect of different cooling conditions for grain size measurement on slab

surfaces. This was the main reason for simulating the austenite grain growth under controlled conditions in the laboratory scale. The development of this experiment will be discussed in detail in the following section.

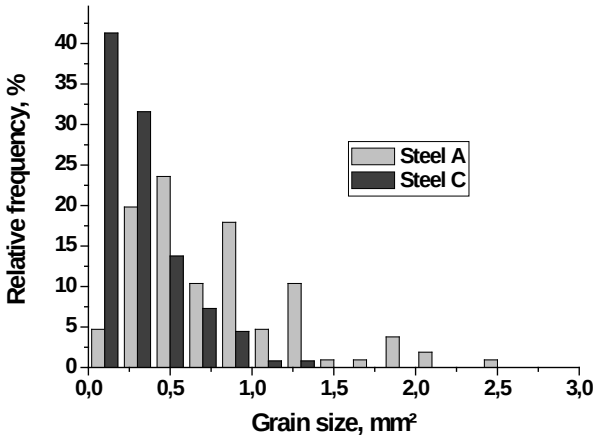

Figure 2: Grain size distribution at the surface for slabs A and C

Experimental simulation of austenite grain growth under continuous casting conditions

As mentioned above, the steel composition and the thermal cycle are the most relevant parameters determining the austenite grain size in the continuous casting process. The cooling of the strand surface in the slab casting process is characterized by a relatively high heat extraction in the mold, a recurrent change of contact with water sprays, rolls and atmosphere within the secondary cooling zone and finally the heat transfer through radiation during the further cooling. It is worth noting that the temperature inside the slab shows higher values with increasing distance from the surface. Therefore the residual time in the existence range of austenite is higher in the middle than at the surface of the slab. Under the given conditions and residual times only temperatures above 1000 °C play a decisive role for austenite grain growth.

The simulation of austenite grain growth on the surface of the slab demands, particularly the simulation of the cooling conditions in the mold. A suitable method is based on the SSCT-test method [24-26], where a coated substrate is submerged into the liquid melt in an induction furnace. The thickness of the coating controls the intensity of heat extraction from the surface of the solidifying steel shell. This results in a similar characteristic of solidification compared to solidification in a mold.

After a dwell time of 30s, shell and substrate emerge from the melt. The different cooling strategies employed are either quenching in water, accelerated cooling under inert gas atmosphere or cooling in atmosphere. After cooling to room temperature, the solidified shell is cut into 16 pieces. Each of these pieces is prepared for metallographic examination and the austenite grain size is determined with the method described above.

The exact control of the thermal conditions during the test is a prerequisite for the analysis of the results. For this purpose, two thermocouples are clamped inside the substrate in order to measure the temperature increase. Another thermocouple is positioned inside the solidifying shell. The measured temperatures serve as input data for a thermal model. A typical calculated cooling curve for cooling in air is shown in Figure 3. The characteristic is similar to the temperature at the surface of the strand in a

continuous casting mold. It can be seen that a definition of one cooling rate is apparently not feasible. However, taking T^{γ} as start temperature, and 1000 °C as temperature after 90s, the average cooling rate would amount to round about 5 °C/s, serving only for a rough classification of our own results in comparison with others.

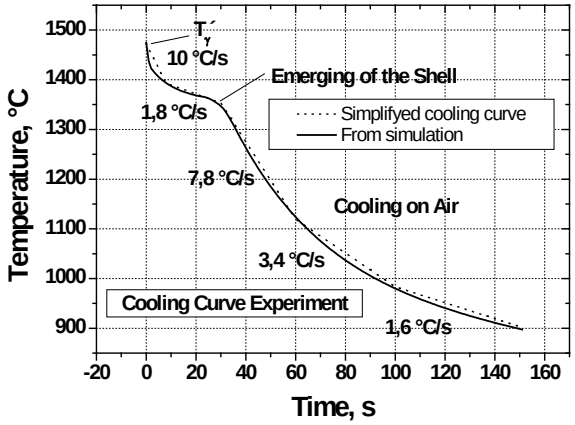

Figure 3: Temperature at the surface of the shell as a function of time for the experiment with subsequent cooling in air.

Besides other test series, one was performed on steel with varying C-content and two groups of Mn-content, one with between 0.30 and 0.38 wt.-% Mn and the second with between 1.04 and 1.88 wt.-% Mn. The composition of these steels together with the calculated equivalent carbon content c_p, the measured grain diameter D in mm and T^{γ}, calculated using the software package IDS, are given in Table II. c_p is calculated using a simplified form of the formula proposed by Howe [27]:

$$c_p = wt.-\%C - 0.14 \cdot wt.-\%Si + 0.04 \cdot wt.-\%Mn \qquad (3)$$

The measured austenite grain size at a distance of 1 mm from the surface versus carbon equivalent can be seen in Figure 4. The results show the expected maximum between a c_p of 0.15 and 0.17 wt.-%. The influence of Mn on grain size seems to be well explained by the equivalent carbon content. The measured values corresponds very well with measured grain size on the slab surface. Again, it should be noticed, that each slab is cast under different conditions.

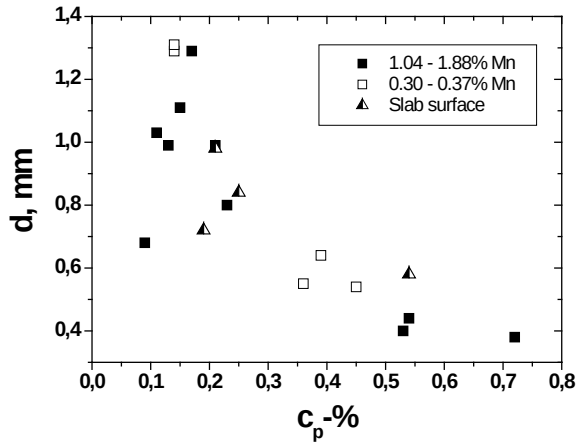

Figure 4: Measured average austenite grain size vs. c_p

Table II. Chemical composition, measured grain diameter and T^{γ} for the experiments						
Test	**C, wt.-%**	**Si, wt.-%**	**Mn,wt.- %**	**cp, wt,-%**	**D, mm**	**T^{γ}, °C**
A1	0,15	0,21	0,31	0,14	1,29	1470
A2	0,15	0,21	0,30	0,14	1,31	1460
A3	0,45	0,18	0,30	0,45	0,54	1416
A4	0,37	0,19	0,38	0,36	0,55	1433
A5	0,40	0,19	0,32	0,39	0,64	1428
B1	0,05	0,25	1,44	0,09	0,68	1432
B2	0,10	0,26	1,46	0,13	0,99	1453
B3	0,20	0,26	1,45	0,23	0,80	1452
B4	0,51	0,27	1,45	0,54	0,44	1391
B5	0,15	0,21	1,04	0,17	1,29	1468
B6	0,16	0,22	1,88	0,21	0,99	1434
B7	0,08	0,30	1,36	0,11	1,03	1474
B8	0,12	0,28	1,34	0,15	1,11	1460
B9	0,51	0,29	1,28	0,53	0,40	1391
B10	0,70	0,25	1,34	0,72	0,38	1358

Grain size prediction model

Normal grain growth in metals and alloys is a diffusion controlled process driven by the reduction in grain boundary energy. Under isothermal conditions the following simplified form of the model proposed by Andersen and Grong [25] describes the grain growth:

$$\frac{dD}{dt} = M_0^* \cdot e^{\left(\frac{-Q_{app}}{RT}\right)} \cdot \left(\frac{1}{D}\right)^{\left(\frac{1}{n}-1\right)} \qquad (4)$$

In this formula M_0^*, a kinetic constant, is assumed to be $4 \cdot 10^{-3}$ $m^2 s^{-1}$[16] and n, the time exponent, 0.5. Q_{app} is the apparent activation energy for grain growth in J/mol, R is the gas constant (8.3145 J/molK) and T the temperature in K. The significant difference between the original model and this simplified formula is the neglect of the pinning forces caused by precipitates. The pinning term is essential for isothermal grain growth calculations. However, under the cooling conditions of the present solidification experiment, precipitates play only a minor role. The high cooling rate and the lacking deformation of the solidifying sample retard the precipitation to temperatures where the grain growth is already marginal. This will be demonstrated in detail later on.

The activation energy Q_{app} serves as the fitting parameter. Using isothermal austenite grain growth measurements from the literature [16, 29, 30] and the results of the solidification experiments, the

following empirical relationship between activation energy and a carbon content above 0.1 wt.-% is determined:

$$Q_{app} = 167686 + 40562 \cdot (wt.-\%C) \qquad (5)$$

Assuming the initial grain size to be in the order of magnitude of the primary dendrite spacing [31], for the present experiment approximately 100µm, and T^{γ} as start temperature for grain growth, the final austenite grain size at the Ar_3-temperature for the temperature development illustrated in Figure 3 was predicted. The calculated versus measured austenite grain size is plotted in Figure 5 using full symbols for the steels in Table II. The correspondence over a wide range of carbon contents is apparent. Only the highest grain size values seem to be underestimated in evidence.

Taking the simple approach from Eq. 2, assuming the initial cooling rate to be 10 °C/s and fitting the first and last constant to the measured results, yields the following equation:

$$\bar{D} = 9.1 \cdot T^{\gamma} - 3152 \cdot \left[\frac{e^{\dot{T}}}{1 + e^{\dot{T}}} \right] - 9044 \qquad (6)$$

The resultant final austenite grain size is plotted in open symbols in Figure 5. It can be seen that the predicted and measured values are also in good agreement. The difference between the original constants and the newly fitted values might be attributed to the different experimental conditions: The original values were valid for cooling rates between 0.5 and 1.5 °C/s, which is quite far below the cooling rates in this experiment. But the deviation points also to an underestimation of the influence of the cooling rate on the final grain size. The validity of Eq. (6) should therefore be limited to initial cooling rates of round about 10 °C/s.

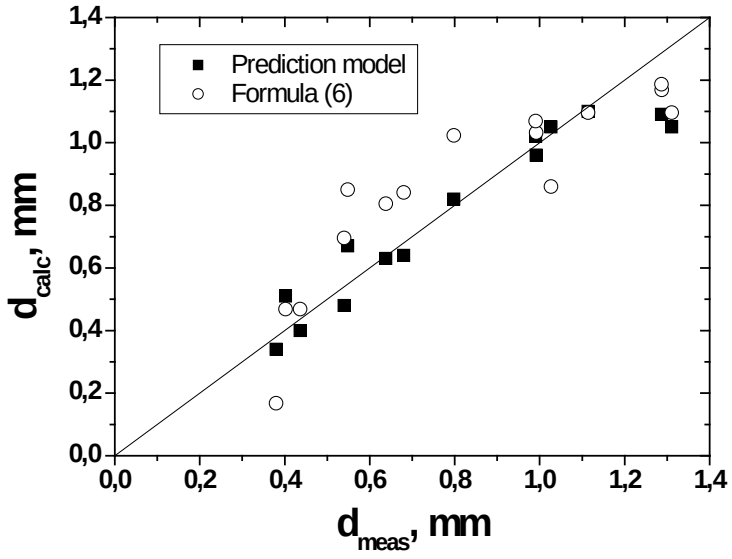

Figure 5: Austenite grain size from the prediction model (Eq. 4) and equation (6) vs. measured average austenite grain size for laboratory tests

As already pointed out, the pinning effect of precipitates was deliberately minimized during the solidification experiment by relatively high cooling rates. A complete elimination of this effect is impossible, as oxides and sulfides may form already in the liquid steel and during solidification. The influence of these inclusions on grain growth should be less important compared with nitrides or carbonitrides. Therefore the influence of any precipitates was neglected in the prediction model. Figure 6 illustrates these conditions: Assuming an equilibrium precipitation temperature of 1100°C, typical for AlN, the pinning effect wound influence the result by less then 5% at the maximum. This simplification afforded the advantage that the activation energy was determined free of the uncertainty about the accuracy of the calculation of particle fractions and particle radii. By the same token, however, the relevance of this simplified model for continuous casting conditions appears limited. Further activities will address the question of the controlled experimental simulation of precipitation and the implementation of these results into the prediction model.

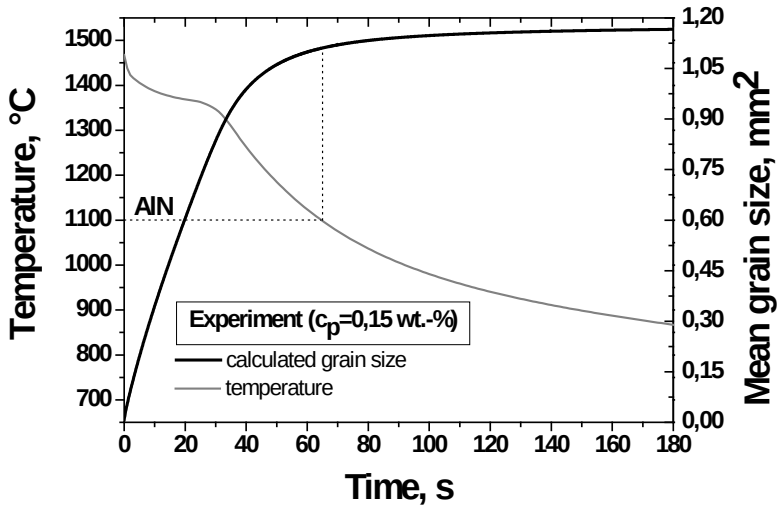

Figure 6: Calculated cooling curve for solidification experiment at 1 mm distance from the surface and calculated austenite grain growth

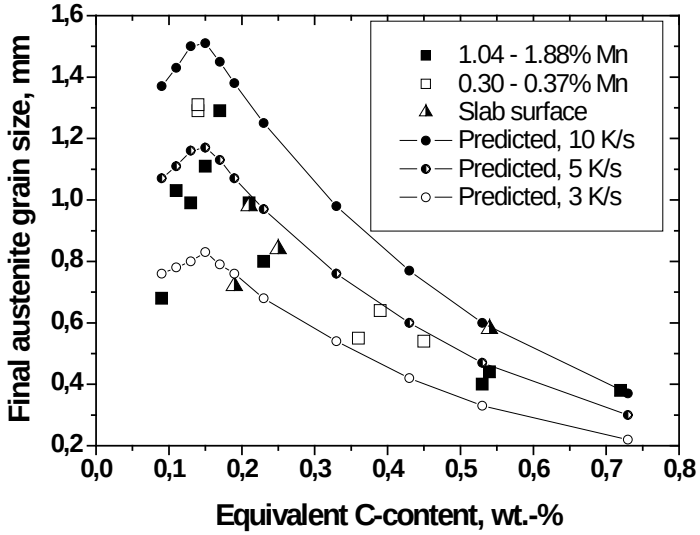

Figure 7: Measured and predicted austenite grain size vs. equivalent casting speed (assumption for predicted grain size: 0.3 wt.-% Si and 1.5 wt.-% Mn, three constant cooling rates)

Figure 7 shows the results of the calculation of the final austenite grain size versus c_p for constant Si-content (0.3 wt.-%) and constant Mn-content (1.5 wt.-%). It can be seen for all three cooling rates that the maximum of the final austenite grain size is determined for the steels containing between 0.15 and 0.17 wt.-%.

Coming back to the topic discussed in the introduction, i.e. the prediction of RA from the austenite grain diameter for a cooling rate of 5 °C/s, the resultant difference between the investigated steels is remarkable: For the simplified assumption that a steel with 0.17 wt.-% c_p and one with 0.4 wt.-% yield the same minimum RA in the ductility trough when the austenite grain size is the same, the difference in the austenite grain size (appr. 1.2 compared with 0.6 mm), would result in an RA lower by 30 to 50 % for the 0.17 wt.-c_p-steel, and, consequently a lower critical strain to prevent surface crack formation.

Although, as already discussed, the prediction model is limited in its relevance for the continuous casting process as the influence of precipitates is not considered, the final austenite grain size for the steels in Table I was calculated on the basis of the individual surface temperatures using a thermal model. The lack of pinning forces in the simple model will result in a too low calculated grain size. For steels A (1.1 mm), C (1.0 mm) and D (0.55 mm), the results correspond surprisingly well. The austenite grain growth is overestimated by appr. 20%. For steel B, the predicted result is clearly too high (1.1 mm).

Conclusion

The present work deals with measurement of austenite grain size on slabs and specimens from laboratory experiments, as well as the adjustment of parameters in a simplified grain growth prediction model.

The measured austenite grain size and grain size distribution on the surface of slabs was the basis for the development of a solidification experiment. This experiment allows the simulation of the initial solidification under conditions closely to the continuous casting process. For the present work, higher cooling rates during further cooling were applied, in order to minimize the influence of precipitates, like nitrides and carbonitrides.

The result of the experiments confirms the results of already published work: A clear maximum was found for a carbon equivalent of between 0.15 and 0.17 wt.-%. An increasing carbon content decreases the final austenite grain size.

In a grain size prediction model, the parameter Q_{app} was fitted on the basis of the measured austenite grain size. This model neglects the influence of pinning forces due to precipitates, and is therefore limited to the conditions of the experiments. The controlled cooling conditions in the experiment result in an excellent correspondence between calculated and measured grain size.

First calculations under continuous casting conditions yielded encouraging results. The controlled investigation of precipitations in the experiment (lower cooling rates, deformation of the solidifying shell) followed by the implementation of a precipitation model, will be future steps within this project.

Literature

1. K. Schwerdtfeger, *Crack susceptibility of steels in continuous casting and hot forming* (Verlag Stahleisen, Düsseldorf , 1994)
2. N.A. McPherson, and A. McLean, *Continuous Casting Vol.8: Transverse Cracking in Continuously Cast Products* (Iron and Steel Society, Warrendale, 1997)
3. B. Mintz, S. Yue, and J.J. Jonas, "Hot ductility of steels and its relationship to the problem of transverse cracking during continuous casting," *International Materials Review*, 36 (1991), no. 5:187-217.
4. Y. Maehara, H. Tomono, and K. Yasumoto, "Effect of Notch Geometry on Hot Ductility of Austenite," *Trans. ISIJ*, 27 (1987), 103-109.
5. P. Deprez, J.P. Bricout, and J. Oudin, "Tensile test on in situ solidified notched specimens: effects of temperature history and strain rate on hot ductility of Nb and Nb-V-microalloyed steels, *Mat. Sci. and Engineering*, A168 (1993), 17-22.
6. M. Suzuki, H. Hayashi, H. Shibata, T. Emi, and I.-J. Lee, "Simulation of transverse crack formation on continuously cast peritectic medium carbon steel slabs," *steel research*, 70 (1999), no. 10:412-419.
7. D.N. Crowther, and B. Mintz, "Influence of grain size on hot ductility of plain carbon steels," *Material Science and Technology*, 2 (1986), 951-955.
8. D.N. Crowther, and B. Mintz, "Influence of grain size and precipitation on hot ductility of microalloyed steels," *Material Science and Technology*, 2 (1986), 1099-1105.
9. Y. Ohmori, and T. Kunitake, "Effects of austenite grain size and grain boundary segregation of impurity atoms on high temperature ductility," *Metal Science*, 17 (1983), 325-332.
10. C. Ouchi, and K. Matsumoto, "Hot Ductility in Nb-bearing High-Strength Low-Alloy Steels," *Transactions ISIJ*, 22 (1982), 181-189.
11. B. Mintz, A. Crowley, R. Abushosha, and D.N. Crowther, "Hot ductility curve of an austenite stainless steel and importance of dynamic recrystallisation in determining ductility recovery at high temperatures," *Material Science and Technology*, 15 (1999), 1179-1185.
12. B. Mintz, R. Abushosha, and A. Cowley, "Preliminary analysis of hot ductility curve in simple C-Mn steels," *Material Science and Technology*, 14 (1998), 222-226.
13. Y. Maehara, K. Yasumoto, H. Tomono, T. Nagamichi, and Y. Ohmori, "Surface cracking mechanism of continuously cast low carbon low alloy steel slabs," *Materials Science and Technology*, 6 (1990), 793-805.
14. K. Yasumoto, T. Nagamichi, Y. Maehara, and K. Gunji, "Effects of Alloying Elements and Cooling Rate on Austenite Grain Growth in Solidification and the subsequent Cooling Process of Low Alloy Steel," *Tetsu-to-Hagane (J. Iron Steel Inst. Jpn.*), 73 (1987), no. 14:1738-1745.
15. J. Miettinen, S. Louhenkilpi, and Lauri Holappa, "Coupled Simulation of Heat Transfer and Phase Transformation in Continuous Casting of Steel," *ISIJ International*, 36 (1996), 183-186.
16. K. Schwerdtfeger, A. Köthe, J.M. Rodriguez, and W. Bleck, *Thin slab casting, Volume 1* (EUR 19409/1 EN, Luxembourg, 2001), 33-48.

17. B. Weisgerber, K. Harste, and W. Bleck, “Phenomenological Description of the Surface Morphology and Crack Formation of Continuously Cast Peritectic Steel Slabs,” *steel research int*., 75 (2004), no. 10:686-692.

18. G. Petzlow, *Metallographisches, Keramographisches, Plastographisches Ätzen* (Materialkundlich-Technische Reihe 1, 6. überarbeitete Auflage, Gebrüder Borntraeger Berlin Stuttgart, 1994), 111-122.

19. S. Bechet, and L. Beaujard, “Nouveau reactif pour la mise en évidence micrographique du grain austénitique des aciers trempés ou trempés-revenus,“ *Revue de Métallurgie*, (1955), no. 10:830-836.

20. P. Baldinger, G. Posch und A. Kneissl, “Pikrinsäureätzung zur Austenitkorncharakterisierung mikrolegierter Stähle,“ *Prakt. Metallogr*., 21 (1991)

21. L. Zhang, and D. Cheng Guo, “A General Etchant for Revealing Prior-Austenite Grain Boundaries in Steels,” *Materials Characterization*, 30 (1993), 299-305.

22. G.F. Vander Voort, *Metallography principles and practice* (The Materials Information Society, 1999), 252-261.

23. C. García de Andrés, M.J. Bartolomé, C. Capdevila, D. San Martín, F.G. Caballero, and V. López, “Metallographic techniques for the determination of the austenite grain size in medium-carbon microalloyed steels,” *Materials Characterization*, 46 (2001), 389-398.

24. C. Bernhard, and G. Xia, “Influence of alloying elements on the thermal contraction of peritectic steels during initial solidification,” *Ironmaking and Steelmaking*, 33 (2006), no. 1:52-56.

25. H. Hiebler, and C. Bernhard, “Mechanical Properties and Crack Susceptibility of Steel during Solidification,” *steel research*, 69 (1999), no. 8+9:349-355

26. C. Bernhard, H. Hiebler, and M. Wolf, “Experimental Simulation of Subsurface Crack Formation in Continuous Casting, *Revue de Métallurgie*, Cahiers d’Information Techniques, (2000), 333-344.

27. A.A. Howe, *Segregation and Phase Distribution during solidification of Carbon, Alloy and Stainless Steels* (EUR 133303, ECSC, Luxembourg, 1991)

28. I. Andersen, and O. Grong, “Analytical Modelling of Grain Growth in Metals and Alloys in the Presence of Growing and Dissolving Precipitates – I. Normal Grain Growth,” *Acta metal. mater.*, 43 (1995), no. 7:2673-2688.

29. M. Militzer, A.Giumelli, E.B. Hawbolt, and T.R. Meadowcroft: Austenite Grain Growth Kinetics in Al-Killed Plain Carbon Steels, *Met. and Mat. Trans. A*, 27A (1996), 3399 – 3409.

30. A.K. Giumelli, M. Militzer, and E.B. Hawbold,” Analysis of the Austenite Grain Size Distribution in Plain Carbon Steels,” *ISIJ International*, 39 (1999), no. 3:271-280.

31. T. Maruyama, M. Kudoh, and Y. Itoh, “Effects of Carbon and Ferrite-stabilizing Elements on Austenite Grain Formation for Hypo-peritectic Carbon Steel, *Tetsu-to-Hagane*, 86 (2000), no. 2:86-91.